actuators

MDPI

Article

A Novel Self-Actuated Linear Drive for Long-Range-of-Motion Electromechanical Systems

Mason Dooley and Xiangrong Shen *

Department of Mechanical Engineering, The University of Alabama, Tuscaloosa, AL 35487, USA
* Correspondence: xshen@eng.ua.edu; Tel.: +1-205-348-6743

Abstract: Obtaining powered linear movement over a long range of motion is a common yet challenging task, as the majority of linear actuators have limited ranges of motion as determined by their functioning mechanisms. In this paper, the authors present a novel belt-based self-actuated linear drive (B-SALD), in which a self-powered moving platform slides on a slotted track with essentially unlimited range of motion (only limited by the length of the track). Unlike the traditional rack-and-pinion mechanism, the B-SALD system uses a double-sided timing belt as the power-transmitting element. With the teeth on its inner surface, the belt interacts with a timing pulley for its own circulation; with the teeth on its outer surface, the belt interacts with a linear rail with parallel slots and drives the translation of the moving platform. The unique functioning mechanism generates multiple distinct advantages: no lubrication is required; the slotted track is simple and inexpensive to manufacture; and it provides an inherent compliance to buffer shock loading. With the experiments conducted on a preliminary prototype, it has been demonstrated that the B-SALD is able to provide accurate positioning and continuous motion control, an overall mechanical efficiency of 70% over the majority of the load range, and the capability of generating large force output in the desired manner.

Keywords: linear actuator; belt drive; electromechanical system

Citation: Dooley, M.; Shen, X. A Novel Self-Actuated Linear Drive for Long-Range-of-Motion Electromechanical Systems. *Actuators* **2022**, *11*, 250. https://doi.org/10.3390/act11090250

Academic Editor: Ioan Ursu

Received: 31 July 2022
Accepted: 25 August 2022
Published: 1 September 2022

1. Introduction

Obtaining powered linear movement is a common task in the development of electromechanical systems. Driving such linear motion can be conducted directly using a linear actuator. For example, a permanent magnet linear motor generates linear force through electromagnetic interaction [1], and fluid power actuators (hydraulic and pneumatic cylinders) [2,3] may also generate linear motion and serve as linear drives. Additionally, a variety of novel muscle-like actuators, such as pneumatic artificial muscle [4–6] and shape memory alloy actuator [7], are linear actuators in nature and thus are suitable for powering linear motion directly. Despite the availability of these approaches, such linear actuators have multiple major limitations that affect their performance and practicality. Except for the permanent magnet linear motor, most linear actuators have short ranges of motion, which is a major limitation to their practical use in linear electromechanical systems. Permanent magnet linear motors, in theory, have unlimited ranges of motion. However, expanding the range of motion of a permanent magnet linear motor requires the corresponding increase in magnetic elements, which comes with increased complexity and cost. Further, the weak force capacity and limited choices of available models also affect the practicality of permanent magnet linear motors in real-world applications.

Due primarily to the weaknesses of linear actuators, the majority of linear electromechanical systems are powered with rotational electromagnetic motors, and the transmission devices in such systems are responsible for converting the rotation from power sources to the desired linear motion. When the desired range of motion is limited (e.g., in a 3D printer), such rotary-to-linear transformation can be conducted with an externally powered system (i.e., unpowered moving load driven by a stationary power source). For example, a toothed

belt (i.e., timing belt), driven by a rotational motor through a pulley, can be used to power a translational load [8]. However, the elasticity and compliance in a toothed belt drive affects the accuracy of positioning and may cause vibration, and thus requires special techniques for motion control [9,10]. Lead screws and ball screws are also used extensively in linear drives [11,12]. Compared with toothed belt drives, lead screw/ball screw drives use rigid elements for the transmission of motion and power, and thus provide high accuracy in positioning. However, the use of rigid elements also increases the inertia of lead screw/ball screw drives, affecting their dynamic responses [11]. As a common problem affecting all externally powered linear systems, their ranges of motion are limited due to the use of motion-transmitting elements (belts or lead screws), as the lengths of such elements cannot increase without limit.

When a large range of motion is required for a linear system, a self-powered drive mechanism becomes the most competitive choice, since such a mechanism provides a consistent performance unaffected by the range of motion. The dominant approach serving this purpose is the traditional rack-and-pinion mechanism, in which the powered rotation of the pinion is converted to its own linear translation when meshing with a stationary rack. A typical application case of the rack-and-pinion mechanism is the stair lift, which requires a heavy load (chair with a human user seated) to be lifted over a long distance [13]. Recently, the authors' group developed a new assistive device to help mobility-challenged individuals in stair climbing, which also utilizes the rack-and-pinion mechanism to power its linear motion [14]. Despite its extensive application in various electromechanical systems, the rack-and-pinion mechanism also has a number of weaknesses. Sufficient lubrication is needed for its smooth operation, and the lubricant on the often-exposed rack may contaminate people's clothing in daily use. The rack is essentially a linear gear, and thus requires accurately machined teeth over the entire length of operation. As such, the long rack needed for a long range of motion is difficult and expensive to manufacture. Further, as a rigid transmission mechanism, the rack-and-pinion mechanism lacks compliance and thus may generate shock loading and affect the user experience during the interaction.

Motivated by the limitations of existing linear actuators (summarized in Table 1), the authors developed a new self-powered linear drive, namely the Belt-based Self-Actuated Linear Drive (B-SALD), which is especially suitable for electromechanical systems with long ranges of motion. Unlike the traditional rack-and-pinion mechanism, the proposed B-SALD system does not rely on the meshing of rigid teeth to transmit force and power. Instead, it uses a double-sided timing belt as the power-transmitting element. With the teeth on its inner surface, the belt interacts with a timing pulley for its own circulation; with the teeth on its outer surface, the belt interacts with a linear rail with parallel slots and drives the translation of the moving platform. Despite the existence of a similar timing-belt-based, self-powered linear drive on the market (ServoBelt [15]), this commercial product has a complex structure and uses a special linear rail with a timing belt bonded to the top surface, making the rail difficult to fabricate at long lengths. The unique functioning mechanism of the proposed B-SALD linear drive provides multiple distinct advantages, including the following: (1) similar to timing belt drives, it does not require lubrication and thus eliminates the lubricant-related contamination problem; (2) the slotted linear rail is easy to fabricate and thus comes with significant cost reduction compared with teethed racks; (3) with the elasticity of the belt, this novel linear drive features an inherent compliance that contributes to the reduction of shock loading and improvement of user experience during the interaction. The configuration and important features of the proposed linear drive are presented in the subsequent section, followed by the prototype demonstration of this novel linear drive approach.

Table 1. Limitations of the existing linear actuators.

Type of Linear Actuator	Major Limitations
Permanent Magnet Linear Motors	Weak force capacity, high cost, and limited choices
Fluid Power Linear Actuators	Mechanically limited range of motion
Artificial Muscle Actuators	Very short range of motion compared with the actuator length
Externally Powered Belt Drives	Low accuracy of positioning and possible vibration due to the elasticity and compliance in the belt
Lead Screw/Ball Screw Drives	Limited range of motion and large inertia associated with the use of rigid screws for power transmission
Rack-and-Pinion Mechanism	Requires sufficient lubrication, long rack difficult and expensive to manufacture, and lacks compliance

2. System Configuration and Functioning Mechanism

As a self-powered linear drive with an electric motor as the power source, the proposed B-SALD system converts the rotation of the motor shaft to the linear motion of the moving platform. Unlike the traditional rack-and-pinion system, the B-SALD system does not rely on the meshing of rigid teeth for the conversion of motion. Instead, a double-sided timing belt, with teeth on both sides, serves as the medium. With the belt's elasticity and flexibility, the B-SALD system can reduce shock loading with its inherent compliance, which is especially useful during the interaction with human users. However, due to the relatively lower force capacity of the timing belt teeth, it is also important to ensure multiple teeth to engage simultaneously for reliable power/force transmission. As shown in Figure 1, the B-SALD system features a flat section of the timing belt such that multiple teeth on the outer surface of the timing belt can engage with the corresponding slots on the linear track simultaneously. To maintain proper tension in the belt, a tensioning pulley is placed at the distant end of the belt drive, which allows the belt tension to be adjusted through the movement of its axle. Further, an additional idler is placed between the driving pulley and the tensioning idler to ensure the reliable tooth-slot contact over the entire length of the straight section. With this unique design, mechanical power can be reliably transmitted from the motor-powered driving pulley to the circulating timing belt, and then from the timing belt to the overall linear movement of the entire moving platform.

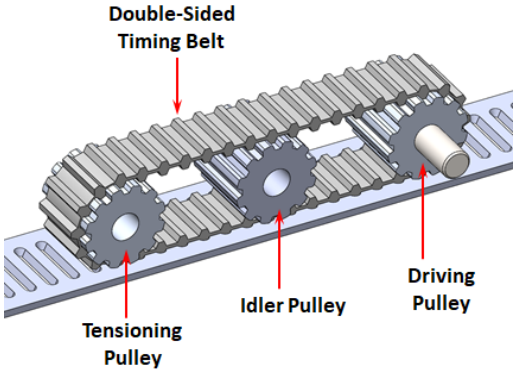

Figure 1. Schematic of the B-SALD functioning mechanism.

3. Prototype Design

To demonstrate the operation of the proposed B-SALD system and to characterize its performance, the authors designed and fabricated a preliminary prototype for experimentation. Two V-slot linear rails (Openbuilds, Zephyrhills, FL, USA) were selected to function as the sliding rails for the moving platform. The platform is supported by multiple V-wheels (from the same manufacturer) mounted at the four corners (Figure 2). To simplify the design of this preliminary prototype, a dual-layered structure was adopted for the design of the moving platform, with two structural plates connected with multiple spacers. The plates also serve as the mounting bases for the three pulleys (the driving pulley, idler

pulley, and tensioning pulley) as well as the electric motor. To reduce the weight and manufacturing cost, the structural plates were fabricated with an aluminum alloy (6061), which is strong and easy to machine.

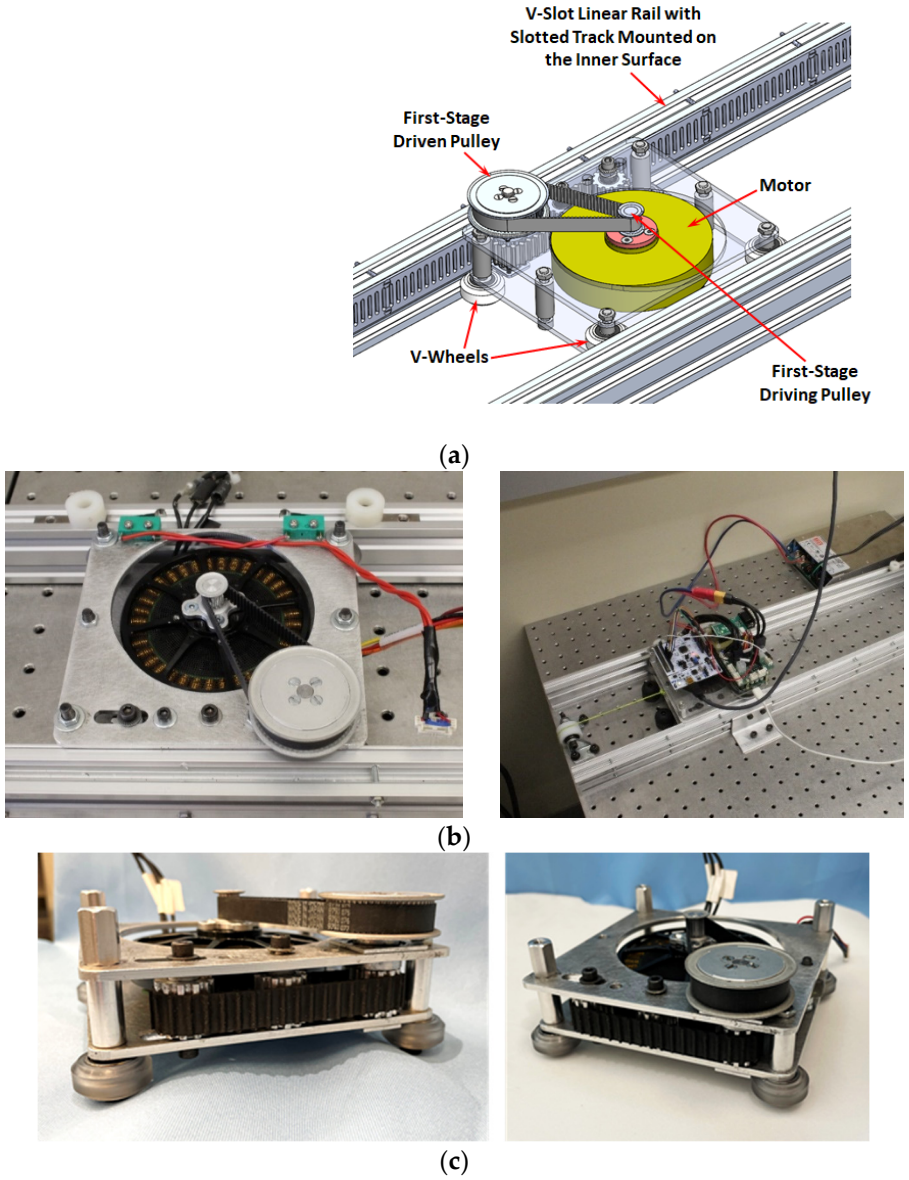

Figure 2. The B-SALD prototype: (**a**) CAD model and the major components; (**b**) photos of the assembled device; (**c**) photos of the driving mechanism of the moving platform.

To obtain large torque output, a disk-shaped motor (U8 Lite-KV85, T-Motor, Nanchang China), originally developed for drones, was selected to power the B-SALD system. The rotation is transmitted to the driving pulley of the B-SALD mechanism through a single-stage timing belt drive, which was selected to provide high flexibility in arranging the mechanical components in the prototype and simplify the design. This first-stage timing belt drive was constructed with a GT2 belt connecting a 15-tooth driving pulley to a 60-tooth driven pulley, providing a 4:1 transmission ratio to amplify the output torque. The output pulley of the first-stage timing belt drive, in turn, is connected to the driving pulley of the B-SALD mechanism, as shown in Figure 3. With the first-stage timing belt placed above the motor and the B-SALD mechanism, the moving platform has a very compact profile, measuring only 121 mm (width) × 127 mm (length) × 50 mm (height).

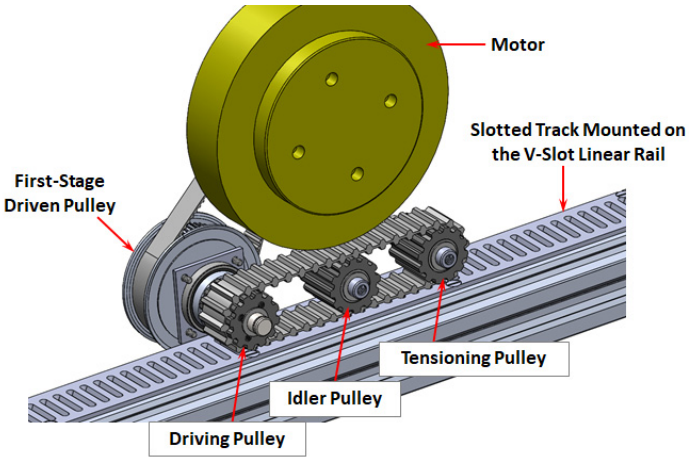

Figure 3. Design details of the B-SALD driving components (bottom view of the prototype).

For the detailed design of the B-SALD prototype, a major challenge was the fabrication of the slots that engage with the timing belt teeth. Considering the large number of slots needed for a long-range linear motion system, an inexpensive method to machine these slots is important for the reduction of the overall cost. Further, as the timing belt teeth need to engage the slots in operation, the compatibility of the slots to the tooth shape is also important. As such, during the detailed design, a standard timing belt model (XL series, SDP/SI, Hicksville, NY, USA) was chosen because of its high strength (130 lbf per 1/8 inch width) as well as its simple trapezoidal tooth profile. Unlike curvilinear teeth, trapezoidal teeth have flat surfaces on both sides. Correspondingly, the mating slots are also shaped in a trapezoidal profile, facilitating the use of simple manufacturing methods such as milling. In the current prototype, an aluminum bar, with parallel slots machined using a chamfer mill, is attached to the inner surface of a V-slot linear rail to serve as the linear component of the B-SALD and engage with the double-sided timing belt for propulsion.

To enable the robotic use of the B-SALD approach, the prototype is also equipped with a magnetic encoder (AS5047P, AMS, Premstaetten, Austria) to measure the motor rotation, which serves as an indirect method of measurement of the linear displacement. The motor control is conducted with a compact digital controller (EPOS4 50/8, Maxon, Sachseln, Switzerland), which communicates with a microcontroller (NUCLEO-L476RG, STMicroelectronics, Geneva, Switzerland) through a CAN bus connection. Leveraging the motor controller's capability of direct current control, the motor torque can be directly commanded for the quantification of the B-SALD's force output. Further, using the measured linear displacement as the feedback, a closed-loop controller can be constructed for the motion control of the B-SALD system, generating the motor current (torque) commands for real-time implementation.

4. Motion Controllers

Similar to the traditional rack-and-pinion system, the B-SALD system belongs to the general category of toothed transmission devices. Unlike friction-based transmission devices (such as flat belt and V-belt drives), the B-SALD can be used for accurate positioning and motion control in electromechanical system. To explore such potential, the authors developed and implemented two typical motion controllers, including a traditional proportional–integral–derivative (PID) controller and a model-based robust (sliding-mode) controller.

4.1. PID Controller

As a common type of controller used extensively in electromechanical systems [16], the PID controller incorporates a derivative term to improve transient response and an integral term to remove steady-state error:

$$i = -K_p e - K_i \int e dt - K_d \frac{de}{dt} \tag{1}$$

where e is the tracking error $e = x - x_d$, x_d is desired displacement, x is the measured displacement, K_p is the proportional gain, K_i is the integral gain, and K_d is the derivative gain.

4.2. Sliding-Mode Controller (SMC)

The standard sliding-mode control technique [17,18] was utilized to develop a model-based robust controller for the B-SALD system. Considering the nonlinear nature of the friction, a model-based controller is expected to better address such nonlinear dynamic behavior. As the basis of this controller, the motion dynamics can be derived by modeling the moving platform as an inertia driven by the actuation force generated by the B-SALD mechanism, subject to the combined viscous and Coulomb frictions:

$$m\ddot{x} + b\dot{x} + c \cdot sgn(\dot{x}) = \frac{m_{tbd} k_A}{r_p} i \tag{2}$$

where i is the motor current (control command), m is the total mass of the moving platform, b is the coefficient of the viscous damping (friction), c is the magnitude of the Coulomb friction, r_p is the radius of the B-SALD driving pulley, m_{tbd} is the transmission ratio of the first-stage timing belt drive, k_A is the torque constant of the motor, and $sgn(\cdot)$ is the sign function defined as

$$sgn(y) = \begin{cases} -1 & when\ y < 0 \\ 0 & when\ y = 0 \\ 1 & when\ y > 0 \end{cases}. \tag{3}$$

For the development of the SMC controller, the sliding surface was defined as $s = \frac{de}{dt} + \lambda e = 0$, where λ is a positive constant known as the control bandwidth. Subsequently, the control law is developed by combining two control components:

$$i = i_{eq} + i_{rb} \tag{4}$$

where the equivalent component i_{eq} is used to obtain the desired behavior on the sliding surface $\dot{s} = 0$:

$$i_{eq} = \left(\frac{r_p}{m_{tbd} k_A} \right) \left[m\left(\ddot{x}_d - \lambda \dot{e} \right) + b\dot{x} + c \cdot sgn(\dot{x}) \right] \tag{5}$$

and the robustness term i_{rb} is used to address the model uncertainties and disturbances:

$$i_{rb} = -\frac{G m r_p}{m_{tbd} k_A} sat\left(\frac{s}{\Phi} \right) \tag{6}$$

where G is the robustness gain, Φ is the boundary layer thickness, and $sat(\cdot)$ is the saturation function defined as

$$sat(y) = \begin{cases} y & when\ |y| \le 1 \\ sgn(y) & otherwise \end{cases} \tag{7}$$

Note that the boundary layer defined by the saturation function in the robustness term is introduced to remove chattering and smooth the control command.

5. Experimental Results

Utilizing the prototype and controllers described above, the authors conducted multiple experiments to quantify the performance of the proposed B-SALD system. The

experiments can be divided into three categories, including motion control experiments, efficiency experiments, and force output experiments.

5.1. Motion Control Experiments

To demonstrate the B-SALD's ability in motion control, related experiments were conducted to quantify its performance in tracking common motion trajectories (step and sinusoidal). Both PID and sliding-mode controllers were implemented and tested. For the implementation of the controllers, the magnetic encoder-measured displacement was digitally differentiated to obtain the required velocity signal, and the control parameters were experimentally tuned to minimize the tracking error.

After implementing and tuning the controllers on the B-SALD prototype, experiments were conducted to quantify the performances in tracking step and sinusoidal functions. Step tracking is used to simulate the common task of positioning. As shown in Figure 4, both the PID and SMC controller provide fast convergence and low steady-state error. Leveraging the dynamic model information, especially the friction model, the SMC is able to provide better positioning accuracy at the steady state. Sinusoidal tracking is used to simulate the common task of obtaining a continuously changing trajectory. As shown in Figure 5, both PID and SMC provide good tracking performance at 0.5 Hz. When the frequency increases to 1.0 Hz, SMC starts to show clear advantage over PID control, with the tracking error consistently kept under 1 mm after the initial transient response (Figure 6). Overall, these experimental results suggest that the B-SALD system, combined with an appropriate control method, is able to provide satisfactory performance of servo control to enable its application in robotics, automation, and other electromechanical systems.

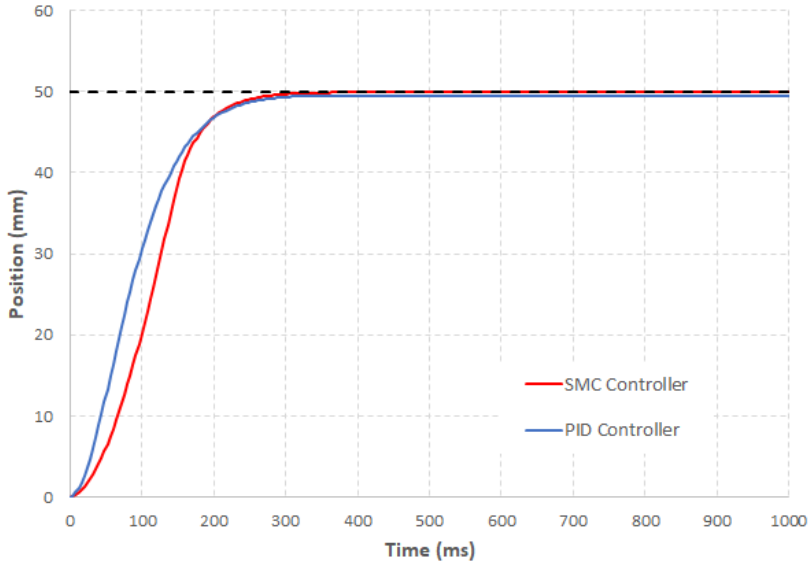

Figure 4. Control performances of the SMC and PID controllers in step tracking.

5.2. Efficiency Characterization Experiments

With the development of the motion controllers above, we also conducted experiments to measure the efficiency of the B-SALD system. To simulate real-world use scenarios, an external weight, suspended with a string, was connected to the moving platform after routing the string through a pulley (Figure 2b). By using different weights, this experimental setup enables the load to be adjusted without excessive complexity. Due to the short range of motion of the prototype, the speed of motion was set at 0.1 m/s in the experiments, i.e., the moving platform was commanded to lift the weight at a constant speed of 0.1 m/s. The input mechanical power is the product of the motor torque and angular velocity. The motor torque was measured indirectly through the current, and its angular velocity was obtained through the differentiation of the magnetic encoder-measured angular displacement. The output mechanical power is the product of the weight of the load and its steady-state linear

velocity. The mechanical efficiency of the B-SALD prototype, defined as output versus input mechanical power, is plotted in Figure 7 as a function of the applied load. Note that the efficiency quantified in the experiments is that of the entire prototype, which is affected by the frictional power loss associated with the first-stage timing belt drive as well as the other related components such as the rollers. When a light load is applied, the frictional power loss is significant, resulting in low efficiency. With the increasing of the load, the efficiency increases and converges to a value of approximately 70%. Considering the power loss associated with other components, the efficiency of the belt-based linear actuation mechanism is expected to be greater than 70%, which can be quantified in future experiments when more accurate instruments are available.

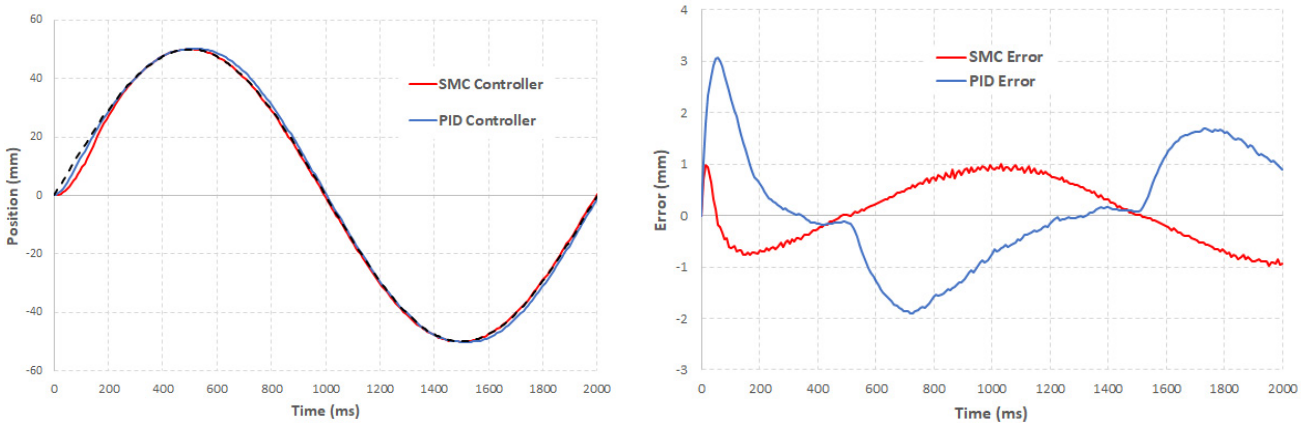

(**a**) (**b**)

Figure 5. Control performances of the SMC and PID controllers in 0.5 Hz sinusoidal tracking: (**a**) comparison of desired (black dashed line) and measured trajectories; (**b**) tracking errors.

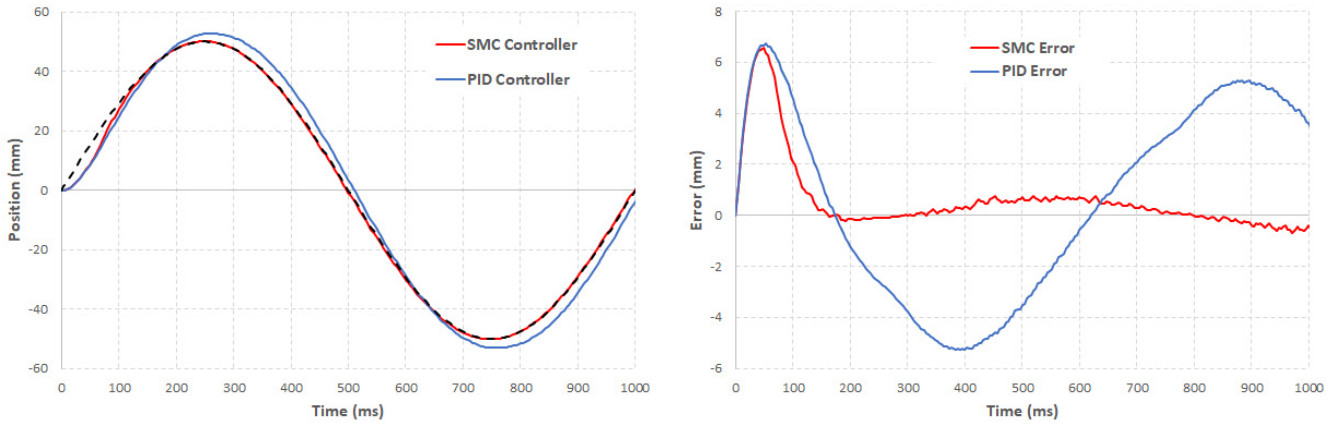

(**a**) (**b**)

Figure 6. Control performances of the SMC and PID controllers in 1.0 Hz sinusoidal tracking: (**a**) comparison of desired (black dashed line) and measured trajectories; (**b**) tracking errors.

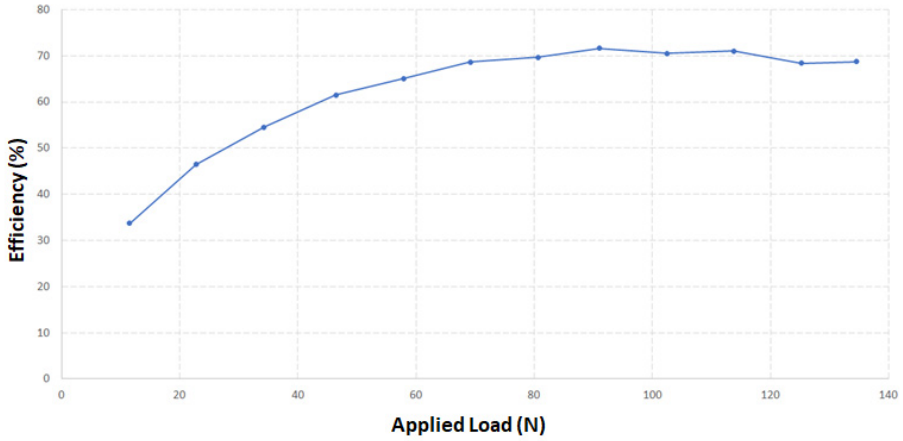

Figure 7. Mechanical efficiency of the B-SALD prototype under different levels of applied load.

5.3. Force Output Measurement

The final part of the B-SALD experiments was conducted to measure the force output as a function of the motor current. To simplify the implementation, the moving platform was attached to a stationary bracket through a bidirectional linear force loadcell (ELPF-500-T3E, Measurement Specialties, Hampton, VA, USA). In the experiments, 10 levels of motor currents were commanded through the motor controller, with the highest value at the motor controller's maximum continuous current (8A). The measured output forces are plotted as a function of the motor current, as shown in Figure 8. As can be observed in this figure, a small dead band exists close to the origin, suggesting that a small amount of motor current is needed to overcome the internal resistance before generating a measurable force output. Except this, the experimentally measured force output closely matches the theoretically predicted actuation force, indicating that the B-SALD is able to produce linear actuation force in the desired way. Due to the limitation of the maximum current imposed by the motor controller, the maximum measured force is 391 N. Based on the peak current of the exterior-rotor motor used in the prototype (reaching as high as 30 A [19]), the B-SALD prototype is projected to produce a peak force of 1.5 kN. Considering the light weight of the moving platform, the B-SALD approach provides a high force-weight ratio, which makes it a competitive choice for powering linear robotic devices (e.g., the aforementioned RailBot system [14]).

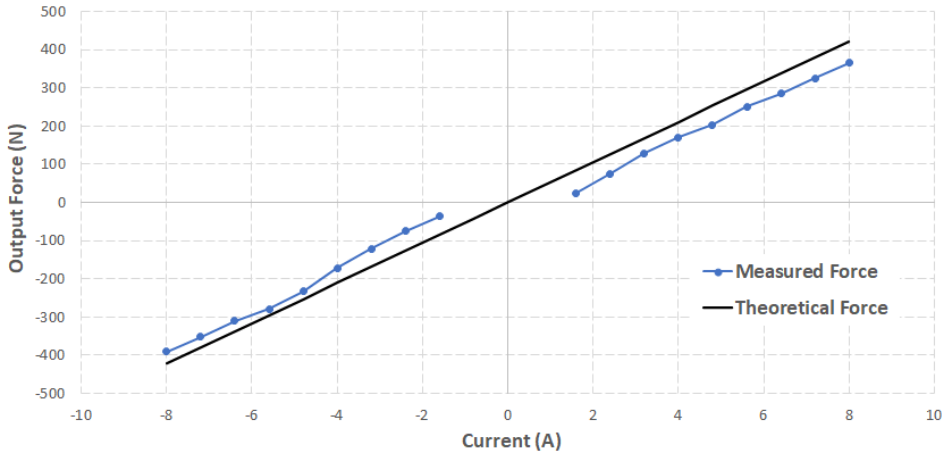

Figure 8. Measured and theoretically calculated output forces of the B-SALD prototype.

For a better understanding of the B-SALD system's performance, a comparison can be conducted against the traditional permanent magnet linear motor and rack-and-pinion system, both of which are capable to providing unlimited range of motion if needed. As a conservative estimation, the force–weight ratio of the B-SALD system can be calculated using the measured maximum force (391 N) and the measured weight of the moving

platform (1.09 kg), generating a value of 359 N/kg. On the permanent magnet linear motor, a recent publication [20] presents the typical force–weight ratio at 23.4 N/kg, which is an order of magnitude lower than the B-SALD system. Further, a linear motor with a long range of motion is expensive to manufacture, as a large number of magnets must be placed over the entire length of its track. For a fair comparison of the B-SALD versus the rack-and-pinion systems, we can construct a hypothetical rack-and-pinion system with maximum commonality with the B-SALD prototype in this paper. Specifically, this rack-and-pinion system can be constructed by replacing the B-SALD mechanism (three pulleys and the double-sided belt as shown in Figure 1) with a single pinion with the same pitch diameter (19 mm) to keep the kinematic performance (maximum speed) unchanged. A pinion meeting such requirement (2664N352, McMaster-Carr, Elmhurst, IL, USA) weighs approximately 63 g, while the total weight of the pulleys and belt it replaces is 37 g. Despite the weight increase of 26 g, such change is only 2.4% of the total weight of the moving platform. As such, it is reasonable to conclude that a rack-and-pinion system has a similar force–weight ratio as a comparable B-SALD system, as the pinion or pulley-belt assembly only takes a small portion of the total weight of the moving platform. Additionally, if the complete system is considered, we can extend the comparison to the structural weight of the stationary components: the rack in the rack-and-pinion system is typically much heavier than the slotted aluminum track in the B-SALD system, because the rack must be made with high-strength metal materials (such as steel) to withstand the heavy load applied to its teeth. For example, a rack compatible with the aforementioned pinion (2485N232, McMaster-Carr, Elmhurst, IL, USA) weighs 449 g for each 500 mm-long section, while the B-SALD's slotted track (in aluminum) weighs only 39 g at the same length. As such, the proposed B-SALD system has a clear advantage with respect to the structural weight, especially when the range of motion is long. Further, the B-SALD's slotted track is much easier and less expensive to manufacture than the rack (essentially a linear gear with accurately shaped teeth), and thus its advantage in system cost is also obvious.

6. Conclusions and Future Work

This paper presents a novel linear drive, namely B-SALD, that generates powered linear translation actuated by an electric motor mounted on the moving platform itself. Unlike most existing linear drives, the self-powered B-SALD approach does not require the use of an externally powered transmission element, and thus the limitation on its range of motion is minimal. The basic mechanism was developed by using a double-sided timing belt as the medium for the transmission of the mechanical power. As multiple teeth on the belt's outer surface engage the corresponding slots on the linear rail simultaneously, the B-SALD can generate a substantial amount of force output in a reliable way. The authors developed a preliminary prototype to demonstrate the B-SALD concept and quantify its performances. Through experiments, it has been demonstrated that the B-SALD system is able to provide satisfactory control performance in positioning and continuous trajectory tracking. The efficiency of the prototype reaches 70% in the majority of the load range, and it is able to produce the actuation force output in the desired way. These results suggests that the B-SALD may become a competitive linear drive approach for electromechanical systems that require powered linear motion and accurate position control for a long range of motion.

Based on the successful demonstration of the B-SALD prototype, the authors plan to further establish a rigorous systematic approach on the design calculation of B-SALD systems. Using finite element analysis, the deflection and stress distribution in the double-sided belt over the entire circumference can be calculated when a certain amount of transmitted force/power is applied. Subsequently, the maximum transmitted force/power can be determined by applying the fatigue failure theory, with the results to be validated through cyclic loading experiments. Additionally, the real-world applications of the B-SALD approach will also be explored, for example, lifting machines (including stair lifts), linear positioning systems, and material handling systems. With the B-SALD's unique

performance, we envision that this novel linear actuation approach can be used in a variety of mechanical systems to make them more functional and affordable.

Author Contributions: Conceptualization, X.S.; methodology: X.S. and M.D.; experiments and analysis: M.D.; writing—original draft preparation: M.D. and X.S.; writing—review and editing, X.S.; supervision: X.S. All authors have read and agreed to the published version of the manuscript.

Funding: This research received no external funding.

Institutional Review Board Statement: Not applicable.

Informed Consent Statement: Not applicable.

Data Availability Statement: The experimental data presented in this study are available on request from the corresponding author.

Acknowledgments: The authors would like to acknowledge Md Rejwanul Haque and Md Rayhan Afsar for their assistance in the experiments.

Conflicts of Interest: The authors declare no conflict of interest.

References

1. Basak, A. *Permanent-Magnet DC Linear Motors*; Clarendon Press: Oxford, UK, 1996; Volume 40.
2. Sato, K.; Sano, Y. Practical and intuitive controller design method for precision positioning of a pneumatic cylinder actuator stage. *Precis. Eng.* **2014**, *38*, 703–710. [CrossRef]
3. Hao, Y.; Quan, L.; Qiao, S.; Xia, L.; Wang, X. Coordinated Control and Characteristics of an Integrated Hydraulic-Electric Hybrid Linear Drive System. *IEEE/ASME Trans. Mechatron.* **2021**, *27*, 1138–1149. [CrossRef]
4. Tondu, B. Modelling of the McKibben artificial muscle: A review. *J. Intell. Mater. Syst. Struct.* **2012**, *23*, 225–253. [CrossRef]
5. Krishnan, G.; Bishop-Moser, J.; Kim, C.; Kota, S. Kinematics of a generalized class of pneumatic artificial muscles. *J. Mech. Robot.* **2015**, *7*, 041014. [CrossRef]
6. Olson, G.; Manjarrez, H.; Adams, J.A.; Mengüç, Y. Experimentally identified models of McKibben soft actuators as primary movers and passive structures. *J. Mech. Robot.* **2022**, *14*, 011006. [CrossRef]
7. Ikuta, K. Micro/miniature shape memory alloy actuator. In Proceedings of the IEEE International Conference on Robotics and Automation, Cincinnati, OH, USA, 13–18 May 1990; pp. 2156–2161.
8. Nevaranta, N.; Parkkinen, J.; Lindh, T.; Niemelä, M.; Pyrhönen, O.; Pyrhönen, J. Online estimation of linear tooth belt drive system parameters. *IEEE Trans. Ind. Electron.* **2015**, *62*, 7214–7223. [CrossRef]
9. Hace, A.; Jezernik, K.; Sabanovic, A. A new robust position control algorithm for a linear belt-drive. In Proceedings of the IEEE International Conference on Mechatronics, Istanbul, Turkey, 5 June 2004; pp. 358–363.
10. Hace, A.; Jezernik, K.; Sabanovic, A. SMC with disturbance observer for a linear belt drive. *IEEE Trans. Ind. Electron.* **2007**, *54*, 3402–3412. [CrossRef]
11. Varanasi, K.K.; Nayfeh, S.A. The dynamics of lead-screw drives: Low-order modeling and experiments. *J. Dyn. Syst. Meas. Control* **2004**, *126*, 388–396. [CrossRef]
12. Jones, M.H.; Velinsky, S.A.; Lasky, T.A. Dynamics of the planetary roller screw mechanism. *J. Mech. Robot.* **2016**, *8*, 014503. [CrossRef]
13. Aead, A.; Rayes, N.; Temraz, R. Design of a Novel Wheelchair Lift. *Eur. J. Eng. Technol.* **2016**, *4*, 6.
14. Afsar, M.R.; Haque, M.R.; Dooley, M.; Shen, X. Railbot: A Novel Assistive Device for Stair Climbing. *J. Med. Devices* **2021**, *15*, 01450. [CrossRef]
15. Bell-Everman. ServeBelt Linear Drive. Available online: https://www.bell-everman.com/products/linear-positioning/servobelt-linear-sbl (accessed on 22 June 2021).
16. Åström, K.J.; Hägglund, T. *PID Controllers: Theory, Design, and Tuning*; Instrument Society of America: Research Triangle, NC, USA, 1995; Volume 2.
17. Slotine, J.-J.E.; Li, W. *Applied Nonlinear Control*; Prentice Hall: Englewood Cliffs, NJ, USA, 1991; Volume 199.
18. Edwards, C.; Spurgeon, S. *Sliding Mode Control: Theory and Applications*; CRC Press: Boca Raton, FL, USA, 1998.
19. Lee, U.H.; Pan, C.-W.; Rouse, E.J. Empirical characterization of a high-performance exterior-rotor type brushless DC motor and drive. In Proceedings of 2019 IEEE/RSJ International Conference on Intelligent Robots and Systems (IROS), Macau, China, 3–8 November 2019; pp. 8018–8025.
20. Boduroglu, A.; Demir, Y.; Cumhur, B.; Aydin, M. A novel track structure of double-sided linear PM synchronous motor for low cost and high force density applications. *IEEE Trans. Magn.* **2020**, *57*, 8201305. [CrossRef]